Eur. Phys. J. Special Topics **226**, 353–363 (2017)

DOI: 10.1140/epjst/e2016-60177-8

THE EUROPEAN PHYSICAL JOURNAL SPECIAL TOPICS

Regular Article

Modelling the dynamics of stem cells in colonic crypts

Sirio Orozco-Fuentes and Rafael A. Barrio[a]

Instituto de Física, Universidad Nacional Autónoma de México, Apartado Postal 20-364, 01000 México D.F., Mexico

Received 10 June 2016 / Received in final form 19 September 2016
Published online 6 March 2017

Abstract. We present a theoretical and computational framework to model the colonic crypt organisation in the human intestine. We construct a theoretical and computational framework to model the colonic crypt behaviour, using a Voronoi tessellation to represent each cell and elastic forces between them we addressed how their dynamical disfunction can lead to tumour masses and cancer. Our results indicate that for certain parameters the crypt is in a homeostatic state, but slight changes on their values can disrupt this behaviour.

1 Introduction

An important problem in developmental biology is to unravel the mechanisms involved in the formation of an organism, such as, how the morphogenetic responses, cell growth and differentiation can lead to a highly organised structure. Recent discoveries have pointed out that failure of these processes during the formation of tissues and organs can lead to a variety of abnormalities such as tumour cell masses and cancerogenesis [1].

In a mature organism, stem cells are in charge of replenishing the epithelial layers that line all organs in the individual. Particularly in the intestinal epithelium, stem cells are the unity in charge of the replenishing of the epithelial monolayer that covers this organ and due to the rapid renewal of this lining there is a high probability of a tumour development and growth which can lead to a formation of cancer.

Therefore, the study of how stem cells can maintain their ability to divide (totipotent) and give rise to daughter cells that differentiate into tissues and organs is fundamental to understanding the development of multicellular organisms and consequently the formation of tumours and cancer. Particularly, cancer has been shown to occur due to gene expression, related to changes in the environment which trigger cellular response, signalling and chemotaxis [2,3].

Since the formation of tumours is a disease connected with mutations in some cells, that continuously produce (*via* proliferation) more progenitor tumour cells [4] some computational models have been developed to study the clonal conversion of the colonic crypt due to the competition between wild-type (healthy cells) and mutant cells at the base of the crypt [5–7].

[a] e-mail: barrio.rafael@gmail.com

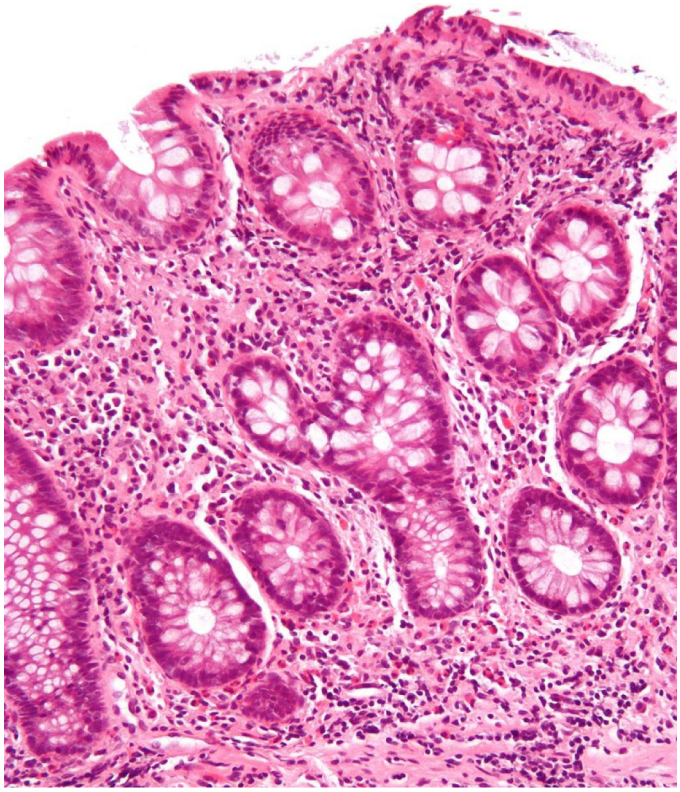

Fig. 1. Micrograph showing intestinal crypts and intestinal crypt branching. ©User:Nephron / Wikimedia Commons / CC-BY-SA-3.0.

The epithelial layer of the human intestine tract is the body's largest mucosal surface, divided into two segments, the small and the large intestine or colon. The small intestine mucosa is composed of a single layer of cells organised in finger-like protrusions, also known as *villi*, and invaginations or crypts of Lieberkühn. The large intestine, on the other side, is only composed of a single layer of cells organised in crypts and there are no villi. Cells lining the intestinal epithelium are replaced every 2–3 days in mice and every 3–5 days in humans [8], making it the most rapidly renewing tissue in the mammalian body and a suitable model for studying adult mammalian stem cells. Since, this tissue is formed by about 2×10^7 crypts, which are "test-tube" shaped invaginations in the epithelium of the colon, they provide a huge surface area for the absorption of water and nutrients while form a protective barrier from harmful substances entering the *lamina propia* [9].

Colonic crypts are tightly packed cylindrical tubes which are evenly distributed within a central hole along the length of the crypt, also known as the crypt lumen, see Figure 1. A human colonic crypt contains approximately 2000 cells, with about 75–110 cells long and an average crypt circumference of 23 cells [10]. Experimental (labelling-index) studies indicate an ordering along the crypt where proliferative cells are located at the base of the crypt and mature cells at the crypt orifice (lumen). Observations of cell proliferation markers suggest a sharp boundary between the proliferative and mature regions, where the proliferative cells occupy the lower third of the crypt [11].

A healthy human colonic crypt contains a population of 5 to 6 stem-cells that reside at or near the base of the crypt [10]. These stem cells divide to produce transit

amplifying (TA) cells which proliferate rapidly and mature as they migrate up the crypt. These TA cells perform several symmetric divisions before finally differentiating. Since only the cells located at the base of the crypt proliferate (due to mitotic activity), this process creates a cell migration up the crypt, resulting in a pressure driven cell flow.

When differentiated epithelial cells reach the crypt collar, they undergo apoptosis and/or are shed into the lumen. In addition to this, a process of programmed cell death, known as *anoikis*, is triggered when there is inadequate adhesion of the epithelial cells to the extracellular matrix [12]. This detachment induces apoptosis (cell death) and under healthy circumstances all these processes combined maintain tissue homeostasis by restricting proliferation to a monolayer and by preventing cells from reattaching and resuming growth in another location.

The establishment of an upward migration and removal of cells inside the crypt gives a defence mechanism against mutated cells, via renewing the epithelial layer every few days. The disruption of the balance in these regulatory processes is linked to the formation of adenomas and carcinomas, see Figure 1. Transit from the crypt base to the surface takes 5–6 days in humans. In the rat's small intestine, experiments have showed that cell velocity increases linearly with the crypt height and exhibits a circadian variation [13]: Cells move at 13 μm/hr at the upper crypt and 34 μm/hr in the base of the *villus*, with this velocity increasing to 51.8 μm/hr in the upper villus (where cells are continuously enlarged) [14].

Colorectal Cancer (CRC) is one of the most frequent cancer disease in the population with one million of new cases every year (worldwide) and with 33% of mortality rate. CRC is thought to originate due to genetic and epigenetic alterations that affect the cellular dynamics of the crypts lining the large intestine. When these genetic mutations occur, cells can accumulate and this alters the cell migration flow velocity, then such cells acquire the ability to persist and multiply inside the crypts [15,16]. It is generally believed that formation of tumours in the colon starts as a disease connected with mutations in stem cells, that continuously produce (*via* proliferation) more progenitor tumour cells [4]. Experimental studies and computational models have been developed to study the clonal conversion of the colonic crypt due to the competition between wild-type (healthy cells) and mutant cells at the base of the crypt [5–7,17].

Therefore, understanding how cells organise themselves inside the crypts is important to gain insight into the origins of adenomas. Disruption of crypt dynamics increases stress on the walls of the crypts and if some stem cell acquire a mutation that increases proliferation, inhibits apoptosis or alter cell-cell adhesion in its progeny, this mutant clone can colonise the entire crypt and replace de non-mutant cell population.

There are many biochemical pathways, whose disfunction lead to genetic mutations in the crypt and their study is of particular importance to assess the origin of colorectal cancer [6,18]. The Wnt signalling pathways have an important role in many biological processes in animals, regulating embryonic development, cell fate determination (canonical), cell movement, tissue polarity (non-canonical) and carcinogenesis. In the normal intestinal epithelium, Wnt signalling pathways maintain self-renewal of intestinal stem cells and progenitor cells via proliferation and differentiation. Wnt signalling pathways are a large family of secreted proteins that act as morphogens and activate receptors on the cell surface which triggers a myriad of events inside the cell, *via* modulating the expression of target genes [19]. In particular, the canonical Wnt signalling has been implicated in the regulation of intestinal stem cells and crypt dynamics. Mutations and aberrant regulation of the Wnt/β-catenin pathway and APC (adenomatous polyposis coli) gene leads to the onset and progression of Colorectal Cancer (CRC) [20].

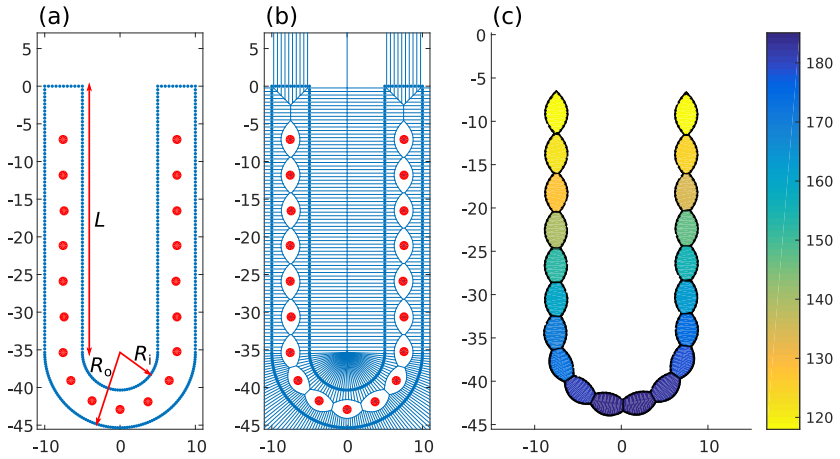

Fig. 2. Crypt domain showing the initial conditions: (a) boundaries (blue points) and cells (red points), R_i, R_o and L are the inner radius, outer radius and length of the crypt, respectively. (b) Voronoi diagram constructed from the previous points and (c) Elastic fields on each cell at the beginning of the simulation.

Dysplastic crypts allow the formation of a benign adenoma if mutated cells persist and proliferate in a localised area. Over time and via accumulated mutations, these growths can progress to a malignant lesion that can break through to the underlying tissue, and thus aid metastasis [21]. It is believed that most cancer result from accumulation of genetic alterations in certain groups of genes, the majority of which are cell cycle regulators, that stimulate or inhibit cell cycle progression. Cell proliferation allows orderly progression through cell cycle, which is governed by proteins known as cyclins and cyclin-dependent kinases. Abnormalities of several cyclins are known to be present in different tumour types.

In this paper we address the important role of Wnt as an external regulator of the dynamics of stem cells in colonic crypts. A spatial gradient of Wnt along the crypt should be result of physical interactions between elastic fields inside the geometric locus of the crypt and the dynamics of proliferation of cells that modifies such elastic fields. In the following section we propose a simple model to test this idea.

2 Dynamical model

Following reference [22], in which we developed a dynamical model for meristems in plants, and taking advantage of the cylindrical symmetry of crypts, we represent cells as Voronoi convex polygons or tessellations, associated with a collection of points in which we assign to each point a limited region of space. All cells are inside a U-shaped two-dimensional domain, bounded by points lying along the boundaries of two semi-circles patched at both open ends with two parallel walls. These boundary points are fixed in space, the interior ones define the crypt lumen, while the exterior ones represent the basement membrane which maintains the integrity and structure of the epithelial layer, giving mechanical support and acting as a physical barrier between the epithelial cells and the connective tissue.

In Figure 2 we show a typical initial condition, that allows to define a row of cells by performing a Voronoi tessellation using a Delaunay triangulation algorithm, see (•) points. A Voronoi diagram, or tessellation, associated with a collection of points (also called seeds, sites, or generators) assigns to each point a limited region of space

in the form of a convex polygon (polyhedron in three dimensions). Voronoi cells are used nowadays in many fields of science, ever since Honda [23] and Saito [24] first proposed the use of 2D Voronoi to model cells in a biological context. For modelling of the colonic crypt, these models were first introduced by Meineke et al. [25]. It is seen that they capture accurately the cell morphology, as a polygonal cell representation which gives the correct tessellation patterns observed in the intestinal epithelium.

Following these previous works, the boundaries in Figure 2 are constructed with 470 points, interspaced at a distance of 0.5 units (blue/small dots). In the same manner, we introduce 19 cells (red/big dots) inside the boundaries, with units, initially spaced at a distance of 5 units. These total 489 points, are used to construct the Voronoi diagram showed in Figure 2b. Once this construction is done, we start the dynamical processes and after 5000 time steps we get the pattern showed in Figure 2, with the cells coloured according to the value of the elastic potential that they have attained. It is important to note that all our simulations are set to last for 50 000 time steps.

Let $\alpha_i (i = 1, 2, ..., N)$ be the area of each cell, and $\mathbf{r}_i$ the positions of the generating points in the initial configuration. It is important to note that the $\mathbf{r}_i$'s are initialised at random. During the dynamical processes, all cells re-accomodate themselves according to the potential from the neighbouring cells or the walls of the crypt. Therefore the vectors $\mathbf{r}_i$ evolve during the dynamics and are updated every time step. It is worth mentioning that these vectors do not necessarily correspond to the centroids of the cells (centres of mass), quantities denoted as $\mathbf{r}_{0i}$, which they are computed as the centre of mass of each cell.

The average quantity $\overline{\alpha}_0 = \sum_{i=1}^{N} \frac{\alpha_i}{N}$ is the area that each cell would have in a regular chain, with each cell's centre of mass located at the same position of their corresponding generators, *i.e.* $d_i = |\mathbf{r}_i - \mathbf{r}_{0i}| = 0 \ \forall i$, which is an equilibrium distance in the regular array. The minimal potential energy corresponds to this equilibrium situation. The quantity d_i, allows us to define a potential energy as deviations from the equilibrium configuration. Irrespective of the form of this function, we could expand it as a Taylor series around equilibrium, and the first non trivial term should be harmonic in the coordinates. Therefore, the equilibrium area $\overline{\alpha}_0$ fixes the size of the mature cells and differences from this value, represent immature cells, this means that deviations from equilibrium are associated with d_i and relaxation of this potential energy assures that cells will tend to have uniform size and isotropic shape. Due to mitotic activity, the distances d_i are modified locally in time, and therefore this represent cells with the wrong shape and size, and consequently largely stressed.

Thereupon, we propose an "elastic potential", acting on each cell i, as [22],

$$V(\mathbf{r}_i, t) = \frac{k_v}{2} \left[\alpha_i(t) - \overline{\alpha}_0(t)\right]^2 + \frac{k_c}{2} \left[\mathbf{r}_i(t) - \mathbf{r}_{0i}(t)\right]^2 \tag{1}$$

where k_v and k_c are appropriate elastic constants. The first term in the right hand side of Equation 1, tends to make the size uniform around the average, and the second one favours a more isotropic the shape for the cells. The forces $\mathbf{F} = -\nabla V$, derived from here are,

$$F_X(X_i, t) = -\frac{k_v}{2} \left[\frac{1}{2} \sum_{m=1}^{M} \frac{(X_i - X_m)\ell_{i,m}}{|\mathbf{r}_i - \mathbf{r}_m|} (\alpha_i - \overline{\alpha}_0)\right] - k_c (X_i - X_{0i}) \tag{2}$$

where $X = x, y$ (the cartesian coordinates), the summation runs over the M neighbouring cells, and we have omitted the time dependency on the right hand side. In

equation (2), $\ell_{i,m}$ denotes the edge length of the m neighbour cell. All the needed quantities can be calculated using the Voronoi algorithm. We account for dissipation in the form of friction due to the inability of cells to make drastic elastic changes of shape an size, using a Stokes's drag force. Adding this term, the total force reads,

$$\mathbf{F}_{\rm tot}(\mathbf{r}_i, t) = \mathbf{F}(x_i, y_i, t) - k\mathbf{v}(\mathbf{r}_i, t) \tag{3}$$

with $\mathbf{v}$ the velocity of the points defining the cell and k a friction coefficient. The N coupled dynamical equations for this system are,

$$\frac{\partial \mathbf{v}}{\partial t} = \frac{1}{m}\mathbf{F}_{tot}, \tag{4a}$$

$$\frac{\partial \mathbf{r}}{\partial t} = \mathbf{v} \tag{4b}$$

which are Newton equations, with m the mass of the cell. These equations can be readily integrated using a simple Euler method, imposing fixed boundary conditions at the fixed surface points, setting the value of the function and its derivative fixed during the calculation. Each coordinate $\mathbf{r_i}$ defining each cell and associated $\mathbf{v_i}$ are calculated and updated at each time step, which is set to $\Delta t = 0.02$, following our previous work in reference [22]. The convergence criteria used [26] which is that the largest element in the Jacobian of the elastic forces are smaller than the dissipation, $\Delta t\, k_c/k \leq 1$.

Cell proliferation and cell cycle arrest

As described in previous sections, normal proliferation of cells inside the crypt is entirely dependent on the stimulation of the Wnt pathway. Therefore, in our model, cells inside the crypt must respond to a source of Wnt in order to proliferate. Absence of this substance should favour cell cycle arrest and terminal differentiation. The cellular mitotic process is modelled with a Lotka-Volterra kinetics between two cyclins (see Ref. [22]), where the period of the cell life cycle is $T = 1/\sqrt{\beta}$, and β is the ratio between the production rate of one substance to the removal of the other. We assume that local concentration of a morphogen, denoted as ω, directly proportional to the elastic field V_i of the cell. Observe that we make the underlying assumption that the Wnt regulating the cell proliferation is directly proportional to the value of ω, so the gradient of V produces the same gradient of Wnt. The concentration of this morphogen Ω in each cell i increases in time as,

$$\frac{d\Omega_i}{dt} = \frac{\beta}{\gamma}\left(\omega_i - \omega_0\right), \tag{5}$$

where γ is a proportionality constant that controls the effect of ω on the cell cycle. Observe that we could have combined the values of the two parameters in only one with appropriate units, but we prefer to keep them separate , so β does not lose its meaning. The parameter ω_0 is a threshold value set to 5×10^{-5} in all simulations. When Ω_i reaches a certain value, we account for cell division in the simulation (mitosis), substituting $\mathbf{r_i}$ by two points oriented at random and at equal distances of $\mathbf{r_i}$. This distance is typically of the order of a quarter of the radius of the cell. Equation (5) is applied to the cell i when the concentration ω_i is greater than the value ω_{cutoff}, which can be tuned to get a variety of behaviours in the simulations. The resulting Voronoi cells alter the local field in the neighbourhood and the extra

Table 1. Values of the dynamical parameters for the time-lapse snapshots shown in Figure 3 and positions of cell divisions and distribution probability shown in Figure 4.

Figure	β	γ	ω_{cutoff}	Features
(a–c)	8	50	0.5	Homeostasis
(d–f)	8	50	0.3	Homeostasis
(g–i)	8	50	0.1	Homeosatsis
(j–l)	28	50	0.5	Accumulation
(m–o)	28	25	0.5	Accumulation

space needed for the two daughter cells is obtained during relaxation by the motion of all neighbouring cells.

When a cell reaches the top of the domain ($y = -5.0$), it is immediately removed and discarded, to simulate apoptosis. This will help conserving the number of cells in the crypt under normal conditions, meaning that one has reached homeostasis.

3 Results

Simulations are carried out varying parameters such as the size of the crypt, number of cells at the initial configuration and the dynamical constants, see Figure 2. Results shown here are obtained by setting $R_{\text{out}} = 10$, $R_{\text{in}} = 5$, $L = 35$ and an initial number of cells $N_c = 19$. With these numerical values, the dynamical constants are set at $k = 3$, $k_v = 20$ and $k_c = 100$ in order to get a homeostatic monolayer tissue, in which the number of cells proliferating at the bottom of the crypt equals the cells leaving the open ends per unit time. The numerical values of the important parameters are shown in Table 1.

Figure 3 shows three snapshots of the simulations (along the same row) for the systems described in Table 1. For Figures 3a–3c equilibrium is always kept and the formed tissue is a monolayer with an homeostatic behaviour, with all divisions occurring near the base of the crypt (dark blue/gray zone). Decreasing ω_{cutoff}, as shown in Figures 3d–3f, results in divisions of cells located at the open ends, see Figure 3e. If we continue decreasing ω_{cutoff} even more, the monolayer phase is lost at times, giving rise to the formation of a bilayer near the base of the crypt, as shown in Figures 3g–3i. Increasing β leads to an agglomeration of cells at the bottom of the crypt, see Figures 3j–3p. For this particular case, the system reaches an equilibrium state, see Figure 3l, since, even though the number of cells dividing at the base is greater, the area required to allocate these new small individuals equals the area of the (bigger) cells leaving the open ends of the crypt. Decreasing ω_{cutoff} leads to cells divisions near the open ends of the crypt, see Figure 4A.

4 Conclusions

The patterning of biological tissues, mediated by morphogens is a dynamic and complex process in which several types of pathways may be involved in such a way that multi-potent cells give rise to the distinct cell types in response to a local concentration. In this work we modelled the Wnt morphogenetic pathway as a quantity directly related to the elastic potential of the simulated cells. Disruption of Wnt, as previously stated, can lead to a myriad of diseases, due to its role as a regulatory signal for other signalling pathways present in the colonic crypts.

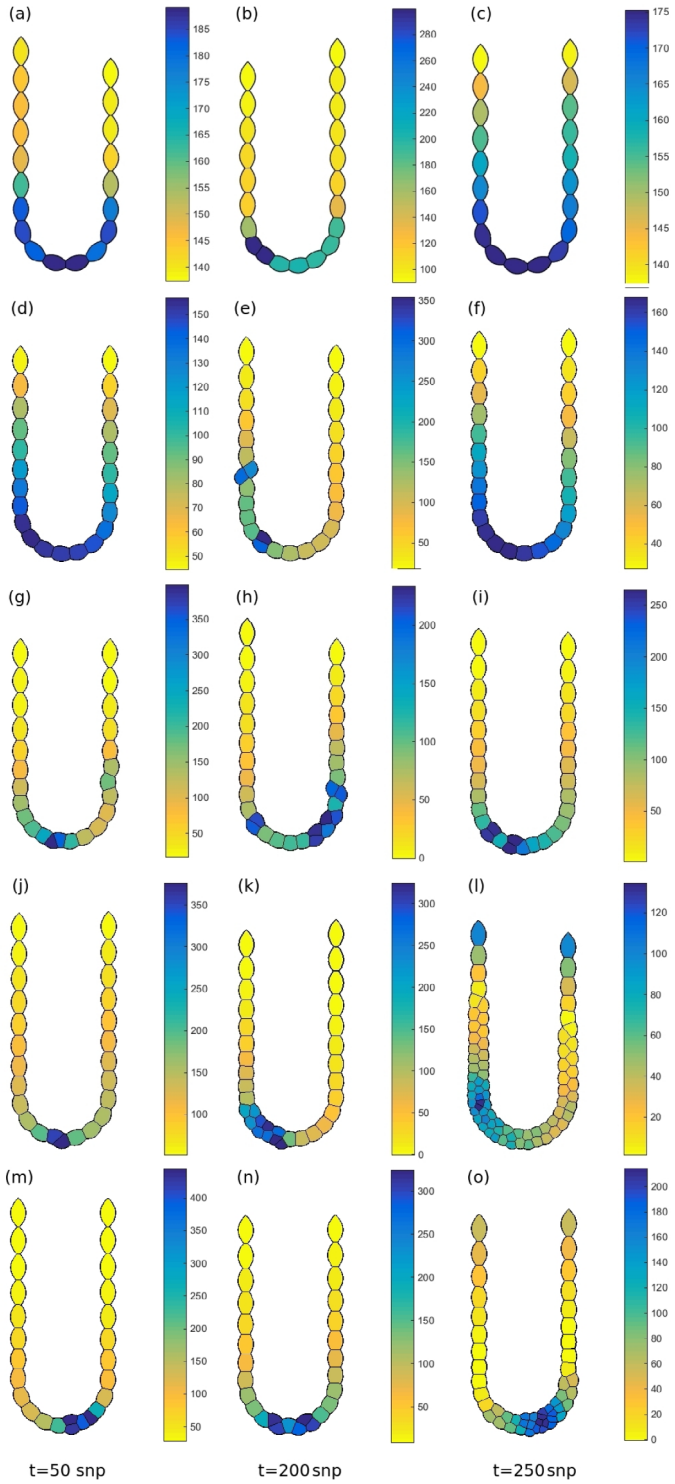

Fig. 3. Snapshots of simulations of the crypt with the parameters shown in Table 1. The time scale factor β controls the form and shape of the morphogen-dependent (ω) tissue growing inside the crypt.

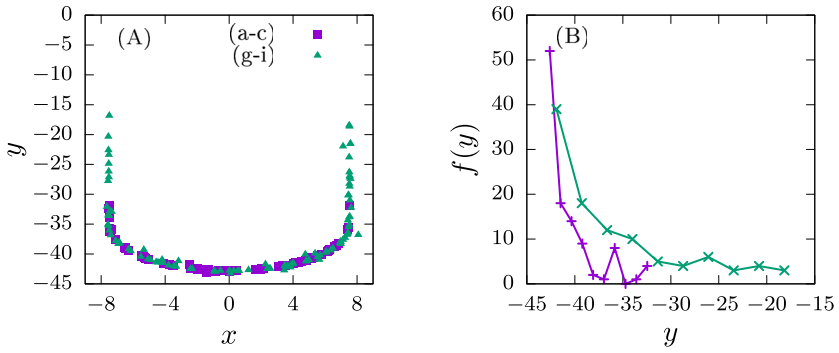

Fig. 4. (A) Coordinates of cell divisions inside the crypt for two different simulations, with the parameters shown in Table 1. Both systems show a steady homeostatic behaviour, but decreasing the value of ω_{cutoff} from 0.5 to 0.1 result in a higher occurrence of divisions near the open ends of the crypt. (B) Distribution function $f(y)$ of the number of divisions against the y-axis of the crypt.

In our simulations, an homeostatic tissue can be observed for the following ranges of the parameters: $\beta = 5 - 20$, $\omega_{cutoff} \geq 0.3$ and $\gamma > 40$. This is an indication of the robustness of the model, since larger perturbations in β and γ are required in order to have "malignant" lesions, such as the ones shown in Figures 3l and 3o. As expected, a decrease in the value of ω_{cutoff} leads to an overreaction of the system, in which cells located near the open ends have a higher rate of divisions. These results imply that a genetic perturbation (through γ) is necessary, in a real biological tissue, in order to develop a malignant lesion. In the same way, changes in the elastic parameters simulate an epigenetic perturbation in the system.

Future work: Morphogene-like gradient of Wnt signal

Wnt signalling pathway is involved in many other organogenesis processes in breast, lung, gut, eyes, kidney, liver, skin, etc. In the case of the colon, this signal also regulates other signalling pathways, such as the Notch pathway (stopping cellular differentiation accordingly) our future aim is to elucidate its sole influence in the crypt using the simplified mathematical model presented in this paper but adding a set of reaction-diffusion equations to model the chemicals inside the crypt.

Morphogens have been widely studied in the literature using reaction-diffusion models, we are introducing the dynamics of this biochemical signal through a set of coupled equations that describe the evolutionary change in concentration of two or more chemicals in a solution. In such a way, the Wnt signalling pathway is going to be represented a substance being attached to the cellular wall *via* a Turing process, using the mathematical model presented in reference [27]. Some important questions to be addressed in our future work is to answer how Wnt signalling regulates cell lineages, giving rise to two different types of secretory cells. It is also important to know what is the interplay between the Wnt signalling and the Notch pathways to stop cellular differentiation along the crypt.

References

1. N. Barker, R.A. Ridgway, J.H. van Es, M. van Wetering, H. Begthel, M. van den Born, E. Danenberg, A.R. Clarke, O.J. Sansom, H. Clevers, Crypt stem cells as the cells-of-origin of intestinal cancer, Nature **457**, 608 (2009)

2. A. d'Onofrio, I.P.M. Tomlinson, A non-linear mathematical model of cell turnover, differentiation and tumorigenesis in the intestinal crypt, J. Theor. Biol. **244**, 367 (2007)
3. I.P.M. Tomlinson, W.F. Bodmer, Failure to programmed cell death and differentiation as causes of tumors: Some simple mathematical models, PNAS **92**, 11130 (1995)
4. P.A. Beachy, S.S. Karhadkar, D.M. Berman, Tissue repair and stem cell renewal in cancirogenesis, Nature **432**, 324 (2004)
5. G.R. Mirams, A.G. Fletcher, P.K. Maini, H.M. Byrne, A theoretical investigation of the effect of proliferation and adhesion on monoclonal conversion in the colonic crypt, J. Theor. Biol. **312**, 143 (2012)
6. S.K. Kershaw, H.M. Byrne, D.J. Gavaghan, J.M. Osborne, Colorectal cancer through simulation and experiment, IET Syst. Biol. **7**, 57 (2013)
7. Y. Kagawa, N. Horita, H. Taniguchi, S. Tsuneda, Modeling of stem cell dynamics in human colonic crypts in silico, J. Gastroenterol. **49**, 263 (2014)
8. B. Creamer, R. Shorter, J. Bamforth, The turnover and shedding of epithelial cells. i. the turnover in the gastro-intestinal tract. Gut **2**, 110 (1961)
9. L.W. Peterson, D. Artis, Intestinal epithelial cells: regulators of barrier function and immune homeostasis, Nature Reviews: Immunology **14**, 141 (2014)
10. A.M. Baker, B. Cereser, S. Melton, A.G. Fletcher, M. Rodriguez-Justo, P.J. Tadrous, A. Humphries, G. Elia, S.A. McDonald, N.A. Wright, B.D. Simons, M. Jansen, T.A. Graham, Quantification of crypt and stem cell evolution in the normal and neoplastic human colon, Cell Rep. **8**, 940 (2014)
11. S.J. Leedham, P. Rodenas-Cuadrado, K. Howarth, A. Lewis, S. Mallappa, S. Segditsas, H. Davis, R. Jeffery, M. Rodriguez-Justo, S. Keshav, S.P.L. Travis, T.A. Graham, J. East, S. Clark, I.P.M. Tomlinson, A basal gradient of wnt and stem-cell number influences regional tumour distribution in human and mouse intestinal tracts, Gut **62**, 83 (2013)
12. S. Frisch, H. Francis, Disruption of epithelial cell-matrix interactions induces apoptosis, J. Cell Biol. **124**, 619 (1994)
13. P. Kaur, C.S. Potten, Circadian variation in migration velocity in small intestinal epithelium, Cell Tissue Kinet. **19**, 591 (1986)
14. S. Tsubouchi, Theoretical implications for cell migration through the crypt and the villus of labelling studies conducted at each position within the crypt, Cell Tissue Kinet. **16**, 441 (1983)
15. D. Cunningham, W. Atkin, H.J. Lenz, H.T. Lynch, B. Minsky, B. Nordlinger, N. Starling, Colorectal cancer, The Lancet **375**, 1030 (2010)
16. X. Liu, J. M., J. Hunt, Kras gene mutation in colorectal cancer is correlated with increased proliferation and spontaneous apoptosis, Am. J. Clin. Pathol. **135**, 245 (2011)
17. A. Humphries, N.A. Wright, Colonic crypt organization and tumorigenesis, Nature Reviews: Cancer **8**, 415 (2008)
18. A.G. Fletcher, P.J. Murray, P.K. Maini, arXiv:1506.05019v1 [q-bio.TO] (2015)
19. O. Voloshanenko, G. Erdmann, T.D. Dubash, I. Augustin, M. Metzig, G. Moffa, C. Hundsrucker, G. Kerr, T. Sandmann, B. Anchang, K. Demir, C. Boehm, S. Leible, C.R. Ball, H. Glimm, R. Spang, M. Boutros, Wnt secretion is required to mantain high levels of wnt activity in colon cancer cells, Nat. Commun. **4**, 13 (2013)
20. P. Polakis, Wnt signaling and cancer, Genes & Dev. **14**, 1837 (2000)
21. C.H.F. Chan, P. Camacho-Leal, C.P. Stanners, Colorectal hyperplasia and dysplasia due to human carcinoembryonic antigen (cea) family member expression in transgenic mice, Plos One **2**, e1353 (2007)
22. R.A. Barrio, J.R. Romero-Arias, M.A. Noguez, E. Azpeitia, E. Ortiz-Gutiérrez, V. Hernández-Hernández, Y. Cortes-Poza, E.R. Álvarez-Buylla, Cell pattern emerge from coupled chemical and physical fields with cell proliferation dynamics: The *arabidopsis thaliana* root as a study system, PLOS: Comput. Biol., **9**, e1003026 (2013)
23. H. Honda, Description of cellular patterns by dirichlet domains: the two-dimensional case, J. Theor. Biol. **72**, 523 (1978)

24. N. Saitô, Asymptotic regular pattern of epidermal cells in mammalian skin, J. Theor. Biol. **95**, 591 (1982)
25. F.A. Meineke, C.S. Potten, M. Loeffler, Cell migration and organization in the intestinal crypt using a lattice-free model, Cell Prolif. **34**, 253 (2001)
26. J. Butcher, *Numerical Methods for Ordinary Differential Equations* (Wiley, 2003)
27. R.A. Barrio, C. Varea, J.L. Aragón, P.K. Maini, A two-dimensional numerical study of spatial pattern formation in interacting turing systems, Bull. Math. Biol. **61**, 483 (1999)